

Analysis on rupture feature of a great complicated earthquake in Kamchatka^{*}

YUAN GAO¹⁾(高原) SI-HUA ZHENG¹⁾(郑斯华) HUI-LAN ZHOU²⁾(周蕙兰)
ZHEN LIU²⁾(刘振) ZHONG-LIANG WU³⁾(吴忠良)

1) *Center for Analysis and Prediction, State Seismological Bureau, 100036 Beijing, China*

2) *Graduate School, University of Science and Technology of China, 100039 Beijing, China*

3) *Institute of Geophysics, State Seismological Bureau, 100081 Beijing, China*

Abstract

The $M_s=7.3$ earthquake of June, 8 1993, off the eastern coast of Kamchatka was very complicated in the rupture history. The rupture feature of this event was discussed by the broadband waveform modelling method as well as the combining analysis on the subevent stack and the quasi-time difference. The results suggest that the rupture propagation of the event was in a strong unidirection and its main rupture processes can be expressed as: rupture nucleation→NEE→near east by north→near east by south→stop, from deep to shallow.

Key words: rupture direction broadband waveform modelling quasi-source time function quasi-time difference

1 The $M_s7.3$ earthquake and its tectonic background

A strong earthquake ($m_b=6.4$, $M_s=7.3$) took place nearly off the eastern coast of Kamchatka peninsula, at 51.219°N and 157.836°E , at 13 hour 03 minute 37.6 second (UTC) on June 8, 1993. For this earthquake, the depth was determined as 81 km by National Earthquake Information Center of United States (NEIC), the CMT depth was 49.1 km by Harvard University, the centroid depth was 86 km from United States Geological Survey (USGS). Kamchatka peninsula is located at the northwest of Circum-Pacific seismic zone and at the convergent juncture of two arcuate sub-belts of the Circum-Pacific seismic zone. The Pacific Plate underthrusts beneath the Eurasian Plate there. The strong activity of volcanos and the formation of island arcs are relative to this kind of motion directly. The distinctive geological tectonics and dynamic feature result in the frequent occurrence of earthquakes and complexity of earthquake rupture in this region (Gao and Wu, 1995; Wu and Zang, 1989).

2 Broadband waveform modelling

Tectonic problem studies based on earthquake distribution and source mechanism have become one of important research branches since 1970's. Presently, some parameters such as CMT are adopted to study tectonic problems. But the broadband seismology method, different from the methods as above, can not only deduce the stress state and source mechanism but also deter-

* Received August 23, 1995; revised July 15, 1996; accepted July 15, 1996.

mine the actual fault plane, and more than that, it has high resolution on inferring source rupture process. The broadband waveform can be used to deduce the rupture history of earthquake in more details than the inversion of long period waveform (Choy and Boatwright, 1981; Choy and Bowman, 1990).

Global Digital Seismograph Network (GDSN), including Chinese Digital Seismograph Network (CDSN), recorded the broadband seismic waveforms of the $M_s 7.3$ earthquake of June 8 1993, off eastern coast of Kamchatka (see Figure 1). Using the observed broadband waveforms recorded at 30 stations which the epicentral distances were all between 30° and 90° , we did the waveform modelling. In this range, the $P+pP+sP$ wave group is of high resolution and reliability to the source rupture process studies. The vertical $P+pP+sP$ broadband waveform was obtained by the convolution of source time function and propagation operator (Choy and Boatwright, 1990). The broadband t^* varying with frequency was used to correct the attenuation (Choy and Cormier, 1986). On the basis of USGS moment tensor inversion, adopting the overlapping method of a sequence of subevents, the forward trial-and-error modelling was performed to obtain the quasi-source time function (qSTF) and broadband theoretical waveform of every station by using the parameters of strike, dip, rake, subevent depth, subevent rise time, subevent drop time, relative amplitude and relative time delay. The qSTFs of stations are given in Figure 2, the qSTFs of stations located at the west of the source (such as the stations of SSE and WMQ) are wider than those of stations located at the east of the source (such as the stations of CBM and VTV). Although the specific shape of every qSTF is different from the others, the essential features of these qSTFs are similar. For most of stations, the observed waveform can be modelled well by 8 subevents. However, it is necessary to point out that the observed waveforms of some stations located at the east of source (such as station VTV) can be modelled well only by 6 subevents, seemly there are some difference from others in qSTFs. This kind of result may come from the method itself, i. e. the forward trial-and-error method. As for the subevens 7 and 8, the qSTFs of stations located at the west of source showed stronger than those at the east of

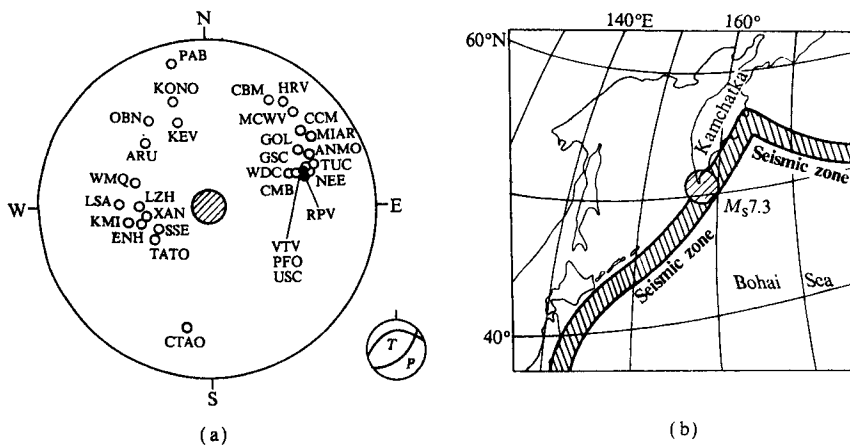


Figure 1 (a) Station distribution and (b) epicentral location

Station locations are given in azimuth and epicentral distance. Station azimuth increases from north clockwise and epicentral distance increases along radius, the circle center is 0° and the outer circle is 100° . The signal \odot (with dashed line in it) and \circ (no dashed line in it) stand for earthquake and station respectively. The source mechanism is shown at the right bottom of Figure(a)

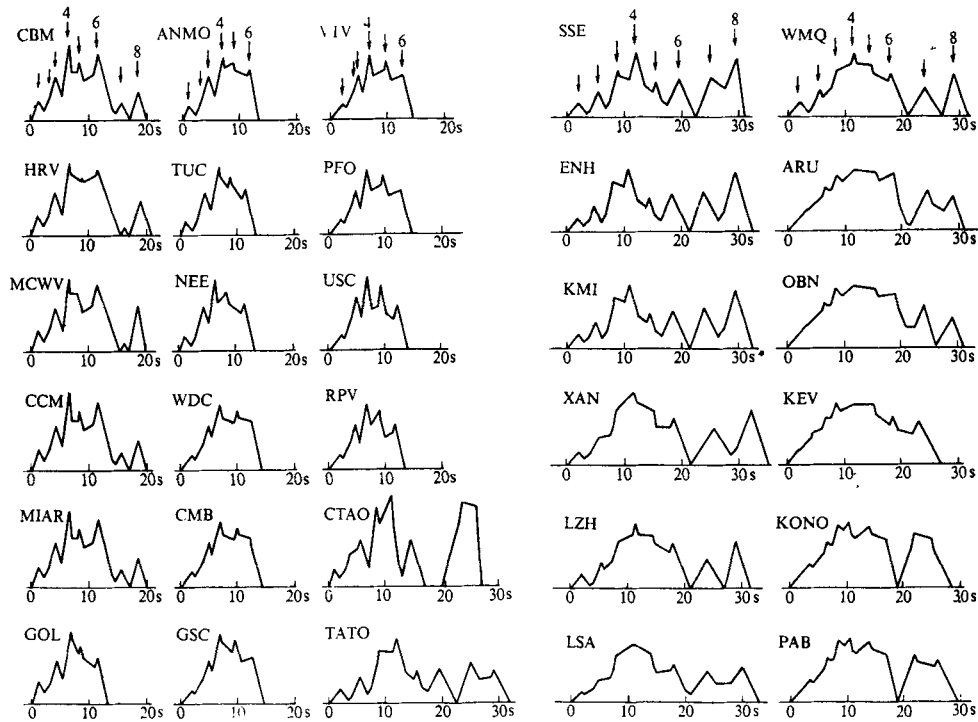


Figure 2 The quasi-source time function

The arrows stand for subevents, alphabets stand for station codes

source. But at least it can be seen that the feature of first 6 subevents is identical for every station in Figure 2. Even in the view of waveform modelling, it is possible that the qSTFs similar to station VTV also have the weaker subevents of Nos. 7 and 8. Strictly, the subevents here should be called as "apparent" subevents, perhaps it is a more rational definition. The modelling results of broadband displacement waveforms are showed in Figure 3.

3 Analysis on source rupture characteristics

For a unilateral source rupture, waveform characteristics are obviously different for receivers with different azimuths (Gao, 1996). If the influence from receiver-source distance is not considered, the widest waveform (e. g. P wave group) will be obtained by the receiver which is in the direction opposite to the direction of rupture propagation, the narrowest waveform will be obtained by the receiver which is in the direction identical to the direction of rupture propagation. For this reason, the actual source rupture direction can be estimated if there is a good distribution of recording stations. In order to reduce the complexity of actual operation on wave modelling, the location parameters of every overlapped subevent is not changed when doing trial-and-error modelling of broadband seismic waveform, so the qSTF of every recording station is obtained and then the actual source rupture direction can be evaluated from the quasi-time differences (qTD) between subevents, which can be seen in qSTFs (see Figure 2). The so-called qTD means the relative interval of rupture times of different subevents observed in every recording station.

The effective qTDs between subevents of every station are shown in the polar coordinates. The qTD value is given along the radius, the center is 0 second. The azimuth of every observation station is same as the angle increasing clockwise from north. The qTD between subevents of every station is drawn in a little black circle (Figure 4). In Figure 4, the dashed line circle means the fit circle of the observed values, the left, middle and right diagrams stand for the qTD pat-

terns of Nos. 1 to 4, 4 to 6 and 6 to 8 subevents respectively. And in each of these three diagrams, the center (C) of the fit circle is biased towards the west. From here, it can be considered that the actual source rupture developed from west to east in general. In order to reduce the possible uncertainty, a kind of sketchy equivalent method is adopted to abstract the essential characteristics. For example, owing to the identical basic feature in qTDs for Nos. 1 to 2, 2 to 3 and 3 to 4 subevents, these three sub-stages may be expressed as one stage (or phase) in pattern in the equivalent method (see the left diagram in Figure 4). This kind of method suggests three successive stages for the $M_s 7.3$ earthquake although there are 8 subevents in station qSTF diagrams. According to the analysis in the above paragraph, the opposite direction (CO) of the deviation direction (OC) of the fit circle center C is the actual deduced direction of source rupture propagation. Thus, the essential rupture pattern of the earthquake in horizontal direction can be obtained: ① Firstly the rupture occurred and formed a rupture extension towards NEE;

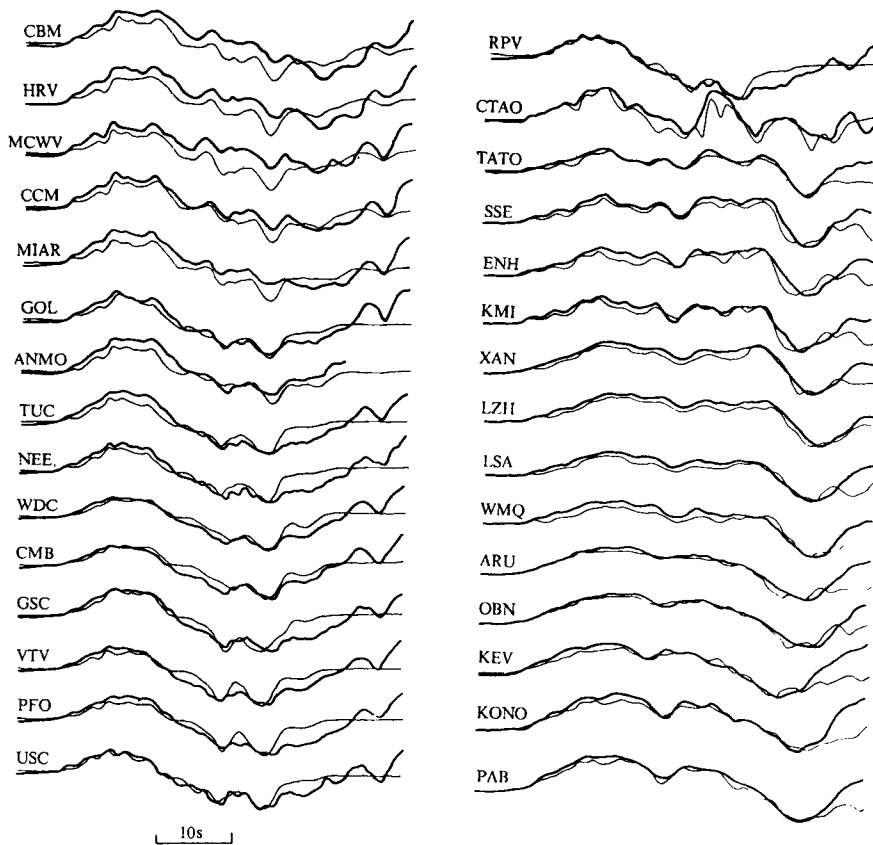


Figure 3 Waveform modelling of vertical broadband recordings

The thick line means the observed waveform, the thin line means the theoretical one

② Secondly the rupture propagation was hindered by some obstacle and turned to near east by north a little; ③ Thirdly the propagation was hindered again, then turned to near east by south a little, and at last stopped. The extensive directions of the rupture are shown at the bottom of every diagram in Figure 4, the DR means the rupture direction, which is signed in the thick black arrow.

To understand the relation of the subevent qTD with the rupture direction better, Figure 5

is drawn with parameters θ (the angle between the station azimuth and the rupture direction) and dt (the subevent qTD). From the fit straight line of dt data, it is seen that the lowest dt value is at about $\theta=0^\circ$ and the highest dt value is at about $\theta=180^\circ$. It has been known that $\theta=0^\circ$ stands for the rupture direction and $\theta=180^\circ$ stands for the opposite direction to the rupture direction. If the α (an angle increasing clockwise from north) is used to mark the rupture direction, α is equal to about 70° , 85° and 95° for the left, middle and right diagrams in Figure 5 respectively.

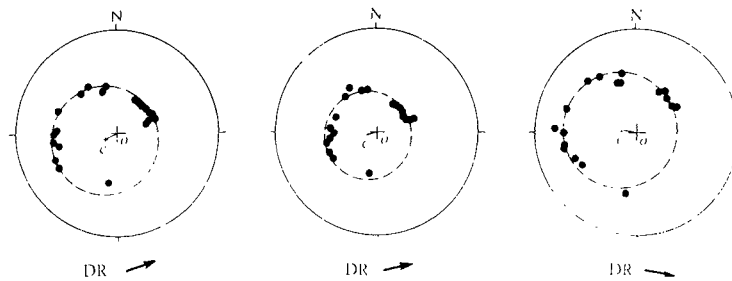


Figure 4 Pattern of rupture propagation from qTD

The qTD for every station is given in a black dot along radius, the circle center is 0 s and the largest radius is 15 s. The angle from north clockwise is the azimuth of station. The left, middle and right diagrams stand for the qTD of Nos. 1 to 4, 4 to 6 and 6 to 8 subevents respectively. For every diagram, the thin inner circle is the fit one of the observed qTD values, the "C" is the center of the fit circle. The thick solid arrows stand for the deduced rupture propagation direction, opposite to the deviation direction of the center C

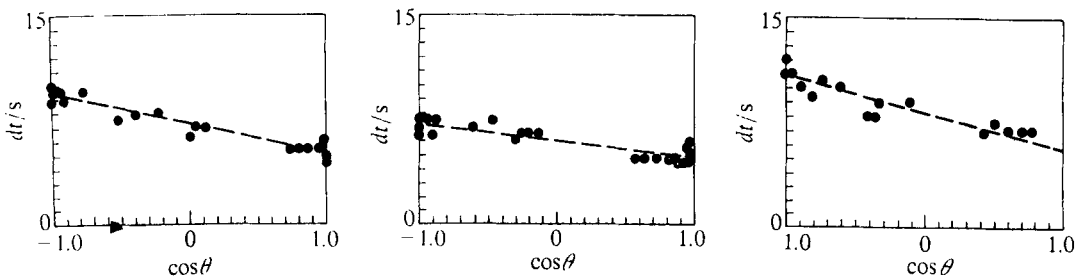


Figure 5 Relation between subevent qTD and rupture direction

The θ means the angle between the station azimuth and the rupture direction clockwise. The dt means the subevent qTD. The dashed lines stand for the fit straight line. The left, middle and right diagrams are corresponding to the situation of Nos. 1 to 4, 4 to 6 and 6 to 8 subevents respectively

From the tectonic feature underthrusting towards NW direction and the source mechanism (see Figure 1), and from the rupture pattern of this earthquake in horizontal direction (Figure 4), it is suggested that the general rupture extended from deep to shallow location for the $M_s 7.3$ earthquake. The result is corresponding to that obtained from waveform modelling in which the depth from subevents of No. s 1 to 8 was basically from deep to shallow. The depth changed from 62 km to 48 km. By analyzing the qSTFs (Gao, 1996), it is known that the widest station qSTF (about 32 s) is about 12 s wider than the narrowest station qSTF (about 20 s). The duration of source rupture can be evaluated to be about 26 s.

From either the broadband P group waveform directly or the obtained qSTFs, an interesting

phenomenon can be found that there is an obvious difference in azimuth for either of them, that is, all stations located at the west of the source had wider waveform (or qSTFs) than those located at the east of the source. This feature provides information for the direct estimation on the rupture direction of earthquake (Gao, 1996). This phenomenon is also corresponding to Zhou's discussion (Zhou *et al.*, 1984) on the relation between the change of the observed waveform width and the rupture propagation direction, in which it was suggested that the multi-rupture and the directive effect of rupture extension made it very complicated for the source process and P waveform of a great earthquake.

4 Results

Advances in broadband seismology have made it possible to study the rupture process of a large or medium-magnitude earthquake in relatively high resolution in a very broad band. Using GDSN (including CDSN) broadband data, to research the earthquake source process of the plate interior and the plate boundary is of important basic significance for recognizing the physical tectonic process and stress field effect of these areas. The rupture history of the 1993 $M_s7.3$ earthquake off the eastern coast of Kamchatka can be obtained by the broadband waveform modelling. According to the optimum double-couple solution of USGS, the earthquake fault plane was that of strike 239° , dip 33° and rake 98° . The main rupture processes can be expressed as: rupture nucleation \rightarrow NEE \rightarrow near east by north \rightarrow near east by south \rightarrow stop, from deep to shallow. The complicated rupture pattern is directly relative to the geological tectonic and the tectonic stress field in this region (Wu *et al.*, 1989, Gao *et al.*, 1995). The rupture propagation of the great $M_s7.3$ earthquake occurred at subduction zone was in strong unidirection. The evaluation, adopted in this paper, on the main characteristic of source rupture is reasonable for the great earthquake of such unilateral rupture.

Great grateful to Professor G. L. CHOY for much help with broadband waveform modelling, thanks to P. CHANG, G. REAGOR and R. NEEDHAM for their kindness and help.

This research was supported by the Chinese Joint Seismological Science Foundation.

References

- Choy G L and Boatwright J, 1981. The rupture characteristics of two deep earthquakes inferred from broadband GDSN data. *Bull Seism Soc Am*, **71**: 691~711
- Choy G L and Cormier V F, 1986. Direct measurement of the mantle attenuation operator from broadband P and S waveforms. *J Geophys Res*, **91**, 7 326~7 342
- Choy G L and Bowman J. 1990. Rupture process of a multiple main shock sequence; analysis of teleseismic, local and field observations of the Tennant Creek, Australia, earthquake of January 22, 1988. *J Geophys Res*, **95**, 6 867~6 882
- Gao Y and Wu Z L, 1995. Rupture process of the 13 November 1993, Kamchatka, $M_s7.1$ earthquake from broadband waveform analysis and its tectonic implications, *Acta Geophysica Sinica*, **38**(1): 79~88
- Gao Y, 1996. A possible simple evaluation of rupture size on strong shock. *Earthquake*, **16**(4): (in Chinese)
- Harvey D and Choy G L, 1982. Broadband deconvolution of GDSN data. *Geophys J R astron Soc*, **69**: 659~668
- Wu Z L and Zang S X, 1989. Distribution and focal mechanism of earthquakes and stress state on Kuril Island and sea of Okhotsk. *Seismology and Geology*, **11**(2): 85~95 (in Chinese)
- Zhou H L Kanamori H and Allen C R, 1984. Analysis of complex earthquakes and source processes of Longling. *Acta Geophysica Sinica*, **27**(6): 523~536 (in Chinese)